MISSOURI S&T

Missouri University of Science and Technology

Scholars' Mine

Electrical and Computer Engineering Faculty Research & Creative Works

Electrical and Computer Engineering

01 Jul 2009

RFID-Based Smart Freezer

Ahmet Soylemezoglu

Maciej Jan Zawodniok
Missouri University of Science and Technology, mjzx9c@mst.edu

Jagannathan Sarangapani
Missouri University of Science and Technology, sarangap@mst.edu

Follow this and additional works at: https://scholarsmine.mst.edu/ele_comeng_facwork

Part of the Computer Sciences Commons, and the Electrical and Computer Engineering Commons

RFID-Based Smart Freezer

Ahmet Soylemezoglu, Maciej J. Zawodniok, *Member, IEEE*, and S. Jagannathan, *Senior Member, IEEE*

Abstract—This paper presents a novel radio-frequency identification (RFID)-based smart freezer using a new inventory-management scheme for extremely low temperature environments. The proposed solution utilizes backpressure inventory control, systematic selection of antenna configuration, and antenna power control. The proposed distributed-inventory-control (DIC) scheme dictates the amount of items transferred through the supply chain. When a high item visibility is ensured, the control scheme maintains the desired level of inventory at each supply-chain echelon. The performance of the DIC scheme is guaranteed using a Lyapunov-based analysis. The proposed RFID antenna-configuration design methodology coupled with locally asymptotically stable distributed power control ensures a 99% read rate of items while minimizing the required number of RFID antennas in the confined cold chain environments with non-RF-friendly materials. The proposed RFID-based smart-freezer performance is verified through simulations of supply chain and experiments on an industrial freezer testbed operating at $-100\ °F$.

Index Terms—Inventory control, low-temperature chemical management, passive radio-frequency identification (RFID), power control.

I. INTRODUCTION

INVENTORY control of time- and temperature-sensitive materials (TTSMs) is a vital problem that needs attention for various industries, for example, composite manufacturers and food producers. Such items have to be stored in a temperature-controlled environment and used within a limited time; otherwise, they become waste. Effective management of TTSM will reduce inventory levels and prevent usage of expired materials, thus reducing costs.

The goal of inventory management is to make the required quantities of items at the right time and location. Currently, in inventory management, barcodes are widely used; however, this technology needs that a line of sight is maintained for the items; besides, the items are scanned one at a time. In addition, barcode-based systems have problems under low-temperature environments. Additionally, tight control of certain item types that are critical for production may be required. Consequently,

tracking of all inventory items through traditional methods may not be economically feasible.

These limitations can be mitigated with radio-frequency identification (RFID) technology, where electronic tags programmed with unique identification code are attached to items. However, in order to provide item-level visibility through monitoring, tracking, and identification of items, a proper RFID implementation is necessary.

The application of RFID to inventory management was discussed in many papers. In [1], inventory management of TTSM using RFID data is presented under ambient-temperature environments. In [2], an RFID-based resource-management system, which integrates RFID, case-based reasoning, and pure integral linear programming, is presented. Lian *et al.* [3] presented the hardware and software issues associated with warehouse logistics control and management system based on RFID in order to improve efficiency. Han *et al.* [4] utilized RFID for accurate localization of mobile robots in automated warehouses for inventory transportation.

The availability of item-level visibility also provides opportunities to control another type of inventory, namely, work-in-process inventory [5]–[7]. In addition, RFID coupled with other sensing schemes helps close the loop on product life-cycle management (PLM) by providing visibility-of-product-related information such as usage data, disposal conditions, etc., from cradle to grave. Jun *et al.* [8] discussed issues regarding PLM, whereas Yang *et al.* [9] develop a component-based software framework for PLM. Within the scope of inventory management, RFID enables smart shelves [9], [10] and smart freezers.

However, the work in [1]–[11] assume that a straightforward deployment of RFID technology providing almost 100% read rates under "controlled" laboratory settings. Upon technology transfer, unforeseen problems, such as readability, may arise from RF interference, RF-absorbing materials, and environmental conditions [12]. For instance, in the proposed smart freezer, the low 100 °F below-zero temperatures cause excessive ice buildup, rendering RFID technology unreliable. In addition, RF-absorbing materials render low read rates and longer reading times.

Therefore, in this paper, a novel scheme of obtaining high read rates within a reasonable reading time for inventory management at extremely low-temperature environments using passive RFID tags is introduced. This overall scheme consists of the following components: 1) a backpressure-based inventory-management scheme for reducing waste and to attain cost savings; 2) a selection scheme for placement and number of antennas inside the freezer; and 3) a locally asymptotically stable distributed-power-control (LASDPC) scheme or simply DPC scheme for antenna transmission in order to obtain a high read

A. Soylemezoglu is with the Department of Engineering Management and Systems Engineering, Missouri University of Science and Technology, Rolla, MO 65409 USA (e-mail: soylemez@mst.edu).

M. J. Zawodniok and S. Jagannathan are with the Department of Electrical and Computer Engineering, Missouri University of Science and Technology, Rolla, MO 65409 USA (e-mail: mjzx9c@mst.edu; sarangap@mst.edu).
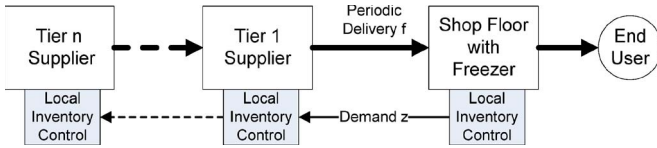
Fig. 1.   Supply chain with backpressure mechanism.

rate required for backpressure-based inventory management. Lyapunov approach [13], [14] is utilized to show the stability of the inventory control and the DPC schemes. The overall method has been experimentally tested and verified on hardware. Both simulation and experimental results are included to justify theoretical conclusions.

II. METHODOLOGY

In this paper, a novel distributed-inventory-control (DIC) scheme for balancing the inventory levels at each layer at a desired target baseline value using the backpressure mechanism along the supply chain is proposed. Fig. 1 shows the supply-chain structure with buffers, for example, freezers on the shop floor, with local inventory-control logic at each layer. This scheme considers only a single type of material flow. However, additional types of materials can be accommodated by using the same control logic for each material. The details of the DIC are presented in Section II-A under the assumption that there is full visibility.

In the subsequent section, antenna-placement and power-control discussion is presented in order to attain the 99%–100% read-rate requirement. The process of selecting the number of antennas and their location is presented in Section II-C. Additionally, a novel mechanism that controls the power of the antennas to reduce the RF interference among them is proposed in Section II-D. The proposed antenna-placement mechanism together with the DPC will be referred to hereinafter as the Missouri S&T scheme, which is shown to reduce the number of antennas inside the freezer while guaranteeing 99% read rates by eliminating all nulls.

The proposed DIC scheme expects a high item visibility. The proposed design methodology attains 99%–100% read rates by considering several factors.

1) The number of antennas and their placements inside the freezer was altered to attain the RF coverage.
2) The power on each antenna is varied using the proposed DPC, which reduces RF interferences and collisions in the backscatter direction.

The design methodology is given in Sections II-B–D.

A. Inventory Management Across the Supply Chain

1) Prediction: This paper proposes a new model to predict the instantaneous demand given by

$$f(k) = [\alpha(k-1)\beta(k-1)] \begin{bmatrix} f(k-1) \\ D(k-1) \end{bmatrix}$$

$$= \theta^{\mathrm{T}}(k-1)\phi(k-1) \qquad (1)$$

where $f(k)$ is the demand at time k, $\alpha(k-1)$ and $\beta(k-1)$ are online-tunable parameters, and $D(k-1)$ is the actual measured demand at the time instant $(k-1)$. The error in prediction is then expressed as

$$e(k-1) = f(k-1) - D(k-2). \qquad (2)$$

Selection of appropriate values for α and β is essential in order to improve the accuracy of the prediction model. Traditionally, these values are selected through offline analysis of historical data. In contrast, the proposed scheme performs online tuning of these parameters to guarantee stability as presented in Theorem 1.

Theorem 1: Consider the instantaneous demand expressed as (1) with the error dynamics given in (2). Let the parameters update be provided by

$$\theta(k) = \theta(k-1) + \gamma\phi(k-1)e(k-1) \qquad (3)$$

where $0 < \gamma < 1$ is the gain factor, then the instantaneous demand approaches the measured value asymptotically.   ∎

Subsequently, the instantaneous value is utilized by the inventory controller to create a backpressure signal z, as shown in Fig. 1. The signal is propagated along the supply chain to adjust the delivery amount periodically. Next, the analysis of the backpressure mechanism is discussed.

2) Backpressure Mechanism in the Supply Chain: In this section, inventory-level dynamics in a supply chain are modeled using difference equations. In order to maintain target inventory levels, the DIC scheme is developed by employing control theory. The performance of DIC is mathematically studied, and the error bound-on inventory level is obtained through the Lyapunov-based analysis.

At a particular echelon j in a supply chain, the inventory level will decrease when materials are used or shipped out to next echelon in the supply chain. When the change depends on the usage, it has to be estimated using (1). Otherwise, the change is dictated by the backpressure signal $z_{i,j-1}$, which indicates the delivery request from the subsequent echelon $j-1$. Then, the demand is fulfilled by delivery f, shipped out from the current echelon of the supply chain. On the other hand, the inventory will increase when the material is delivered from the supplier up the supply chain based on demand z_{ij}. Thus, in a supply-chain environment, the inventory levels change due to the fluctuation in demand.

Overall, the change of the inventory level inside a freezer in the supply chain at echelon j can be expressed as

$$q_{ij}(k+1) = \mathrm{Sat}_Q\left[q_{ij}(k) + z_{ij}(k) - f_{ij}(k) + e_{dij}(k)\right] \quad (4)$$

where $q_{ij}(k)$ is inventory level at freezer i at time k, $z_{ij}(k)$ is the required delivery for freezer i for period k, $f_{ij}(k)$ is the usage rate of the freezer I, and Sat_Q is saturation function modeling the limited capacity of freezers. The fluctuation in the demand $e_{dij}(k)$ is due to many factors, for example, just-in-time manufacturing, machine breakdown, etc.

Remark 1: In a supply chain, a negative delivery size $z_{ij}(k)$ corresponds to a reduction in supply from the baseline level. Reduction is necessary to minimize wastage.   ∎

At any time instant, materials inside the freezer will be shipped back to the supplier. Hence, the calculated delivery request is modified to exclude this case, and actual delivery request $z'_{ij}(k)$ can be expressed as

$$z'_{ij}(k) = \begin{cases} z_{ij}(k), & \text{if } z_i(k) > 0 \\ 0, & \text{if } z_i(k) \leq 0. \end{cases} \quad (5)$$

Remark 2: In the case when $z_{ij}(k)$ is positive, the baseline will be completed with the instant demand. In contrast, for the case of negative $z_{ij}(k)$, there will be no shipment; hence, the inventory-level error cannot be directly controlled. ∎

Define the desired level of inventory as q_{tij}. Then, the error in inventory level is equal to $e_{ij}(k) = q_{tij} - q_{ij}(k)$. This value at the next time instant can be obtained as

$$e_{ij}(k+1) = q_{tij} - q_{ij}(k+1)$$

$$= e_{ij}(k) - z_{ij}(k) + f_{ij}(k) - e_{dij}(k). \quad (6)$$

The requested delivery level $z_{ij}(k)$ should minimize the error in inventory level for the next time instant. In other words,

$$q_{tij} - [q_{ij}(k) + z_{ij}(k) - f_{ij}(k) + e_{dij}(k)] = 0. \quad (7)$$

Unfortunately, the exact demand $f_{ij}(k)$ is unknown for the time period k (future) due to uncertainties such as usage rates, etc. By using an estimated demand value, backpressure control signal can be obtained as

$$z_{ij}(k) = \left[\hat{f}_{ij}(k) + k_v e_{ij}(k) \right] \quad (8)$$

where $\hat{f}_{ij}(k)$ is the predicted demand for the freezer i during the time interval k in echelon j. Then, the expected error in inventory level at time $k+1$ is equal to

$$e_{ij}(k+1) = q_{tij} - q_{ij}(k+1)$$

$$= e_{ij}(k) - k_v e_{ij}(k) + \tilde{f}_{ij}(k) - e_{dij}(k) \quad (9)$$

where $\tilde{f}_{ij}(\cdot) = f_{ij}(\cdot) - \hat{f}_{ij}(\cdot)$ is an error in demand prediction. Next, the bound-on error in inventory level is shown.

Theorem 2 (General Case): Consider the desired inventory level q_{tij} to be finite and the demand-fluctuation bound e_{dM} to be equal to zero. Let the delivery quantity for (4) be given by (8) with the delivery quantity being estimated properly such that the approximation error $\tilde{f}_{ij}(\cdot)$ is bounded above by f_M. Then, the inventory-level backpressure system is uniformly ultimately bounded, provided that $0 < k_v < 1$.

Proof: Consider Lyapunov function candidate $J = [e_{ij}(k)]^2$. Then, the first difference is

$$\Delta J = \left[k_v e_{ij}(k) + \tilde{f}_{ij}(k) + e_{dij}(k) \right]^2 - [e_{ij}(k)]^2. \quad (10)$$

The stability condition $\Delta J \leq 0$ is satisfied if and only if

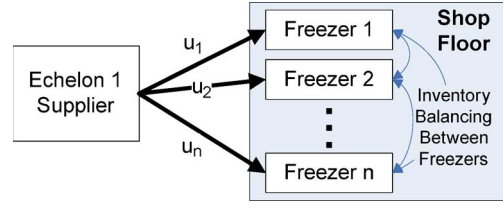$$\|e\| > (f_M + d_M)/(1 - k_{v\max}). \quad (11)$$

Fig. 2.　Inventory balancing between multiple freezers.

When this condition is satisfied, the first difference of Lyapunov function candidate is negative for all k. Hence, the closed-loop system is uniformly ultimately bounded. ∎

Remark 3: The bound-on error in inventory level depends on $k_{v\max}$, as shown in (11). The bound decreases as $k_{v\max}$ approaches zero, thus yielding a smaller error. ∎

Remark 4: Theorem 1 demonstrates that the actual inventory level converges close to the target value, provided that the errors in demand estimation and variation are bounded. ∎

3) Multifreezer Environment: In a typical industrial environment, there may be more than one freezer, as shown in Fig. 2. Then, the overall inventory of the shop floor is expressed as a set of equations given by (4), where $i = 1, \ldots, n$. For simplicity, the following vector form represents the shop-floor inventory levels at echelon j:

$$Q_j(k+1) = Q_j(k) + Z_j(k) + F_j(k) + D_j(k) \quad (12)$$

where

$$Q_j(k) = \begin{bmatrix} q_{1j}(k) \\ q_{2j}(k) \\ \vdots \\ q_{nj}(k) \end{bmatrix} \quad Z_j(k) = \begin{bmatrix} z_{1j}(k) \\ z_{2j}(k) \\ \vdots \\ z_{nj}(k) \end{bmatrix}$$

$$F_j(k) = \begin{bmatrix} f_{1j}(k) \\ f_{2j}(k) \\ \vdots \\ f_{nj}(k) \end{bmatrix} \quad D_j(k) = \begin{bmatrix} e_{d1j}(k) \\ e_{d2j}(k) \\ \vdots \\ e_{dnj}(k) \end{bmatrix}. \quad (13)$$

In such a case, the error in inventory at the shop floor $e(k)$ is equal to the sum of error magnitudes at each freezer

$$e_j(k) = \sum_i |e_{ij}(k)|. \quad (14)$$

4) Inventory Balancing: In the multifreezer scenario, as shown in Fig. 2, items can be quickly moved between the freezers to balance inventory and minimize wastage, thus saving cost. Due to the colocation of freezers, the load-balancing mechanism can yield almost immediate (relative to delivery period) correction of inventory levels among freezers, thus reducing wastage.

In the case of load balancing, the individual inventory levels and the demand and the delivery/usage levels for all freezers can be combined as

$$q_{Tj}(k) = \sum_i q_{ij}(k) \qquad z_{Tj}(k) = \sum_i z_{ij}(k)$$

$$f_{Tj}(k) = \sum_i f_{ij}(k) \qquad e_{dTj}(k) = \sum_i e_{dij}(k) \quad (15)$$

where $q_{Tj}(k)$ is total inventory level on the shop floor at time k for echelon j, $z_{Tj}(k)$ is the corresponding total demand, $f_{Tj}(k)$ is the total usage or delivery shipped out of the current supply-chain level, and $e_{dTj}(k)$ is the total variation of the demand. Therefore, (12) can be written as

$$q_{Tj}(k+1) = q_{Tj}(k) + z_{Tj}(k) - f_{Tj}(k) + e_{dTj}(k). \quad (16)$$

The load balancing is performed internally in order to minimize inventory errors at each freezer. Consequently, the total error in the inventory level at the echelon j is given by $e_{Tj}(k) = q_{Ttj} - q_{Tj}(k)$. In the case of individual inventory controllers, the demand z is fulfilled only when it is a positive value. To prevent excess inventory being shipped back, shifting the load between the freezers can offset the negative demand z as explained next.

First, consider the total demand at echelon "j." In the case of independent inventory control at each freezer, the total demand $z_{T\_NLB,j}(k)$ would include only the positive demand values of the individual freezers at that echelon. In contrast, in the case of inventory balancing, the total demand will include the negative demand as well, which in turn will reduce total demand $z_{T\_LB,j}(k)$ as

$$z_{T\_NLB,j}(k) = \sum_{i,z_i(k)>0} z_{ij}(k) + \sum_{i,z_i(k)\leq0} 0 = \sum_{i,z_i(k)>0} z_{ij}(k)$$

$$z_{T\_LB,j}(k) = \sum_{i,z_i(k)>0} z_{ij}(k) + \sum_{i,z_i(k)\leq0} z_{ij}(k). \quad (17)$$

When there is no negative demand, i.e., $\sum_{i,z_i(k)\leq0} z_{ij}(k) = 0$ for all $j = 1, \ldots, m$, the total demand is equal for both scenarios. However, if there is at least one freezer with negative demand, the corresponding excess inventory will be used to fulfill the positive demand of the other freezers at that echelon, thus reducing the total order or target demand. Thus, the total order in the case of load-balancing scenario will be smaller or at least equal to the total demand observed in the case of no-load balancing. This total demand satisfies

$$0 \leq \sum_{i,z_i(k)\leq0} z_{ij}(k) \Rightarrow z_{T\_LB,j}(k) \leq z_{T\_NLB,j}(k). \quad (18)$$

By using (17) and (18), it can be shown that the load balancing can reduce the total error in the inventory levels corresponding to the negative demand $z_{Tj}(k)$ by shifting inventory among the freezers. In contrast, without load balancing, wastage due to excess inventory at one freezer cannot be redirected to the freezers needing inventory. Additionally, the errors due to demand variation at the freezers may cancel each other out. For instance, in the worst case scenario, the individual errors will be equal for both scenarios, with and without load balancing.

In other words, the total error in inventory levels for load-balancing scenario is smaller or equal to the scenario when the total error in inventory levels without load balancing as

$$\sum_i |e_{ij}(k)| \geq \left|\sum_i e_{ij}(k)\right|. \quad (19)$$

B. Space for Antennas in a Freezer

Initial experiments have demonstrated that the number of antennas and their orientation affect the read rates besides reducing capacity due to antenna placement. However, such problems can be easily overcome by reducing the number of items in the baseline when the 99% visibility is ensured. At present, the freezers are filled up regardless of real usage, thus leading to high baselines and more wastage.

Full visibility through improved read rates allows more accurate usage levels and less waste. However, if for any reason such high baselines are needed, the Missouri S&T smart-freezer scheme can still provide 99% read rates for a fully loaded freezer.

C. Antenna Configuration

The selection process for finding the necessary number of antennas and their localization inside the freezer in order to achieve full visibility is shown in Fig. 3. First, a realistic RF coverage pattern has to be obtained for the utilized antennas in the target environment. Next, the individual antenna coverage pattern is used to determine the number and positions of antennas that provide the RF coverage of the entire freezer cavity. The selection of location and the number of antennas required for attaining such high read rates with low reading times is performed iteratively by adding and positioning one antenna at a time. When the final antenna configuration is acquired, hardware tests can be used to verify that each antenna reads all the tags within its designated area. Finally, the proposed power-control scheme is applied online in order do minimize interference among the antennas while ensuring the desired coverage inside the freezer. The proposed scheme to obtain antenna configuration is described next.

1) Acquisition of Antenna Radiation Pattern: First, an ideal radiation pattern is calculated and modeled by assuming no obstructions and interference. Next, the propagation model is used to calculate the coverage in a nonideal environment. The radiation pattern can be obtained from antenna vendor, through measurements in an anechoic chamber or by using existing models from the literature [15]. For example, a dipole antenna radiation pattern can be calculated [15] using $E_{\text{dipole}}(\theta, r) = -jI_0 e^{j(\omega t - kr)} \sin\theta/(2\pi\varepsilon_0 cr)$, where E_{dipole} is far electric field (or radiated electromagnetic field) of a half-wave dipole at point A, θ is an Euler angle between direction of dipole and the direction to point A, r is the distance between the dipole and the point A, I_0 is the maximum current passing through the dipole, ε_0 is the permittivity of vacuum, c is speed of light in vacuum, λ is wavelength, $\omega = 2\pi F$ is the pulsation at frequency F, and $k = 2\pi/\lambda$ is wavenumber. The radiation patterns are utilized to determine the antenna gains which are subsequently used to study the attenuation caused by the freezer walls, the material of the stored items, and the freezer cavity. This information will be further used to study the overall coverage and nulls and, thus, to determine the number of antennas.

The maximum coverage around an antenna is calculated using signal-strength equation as

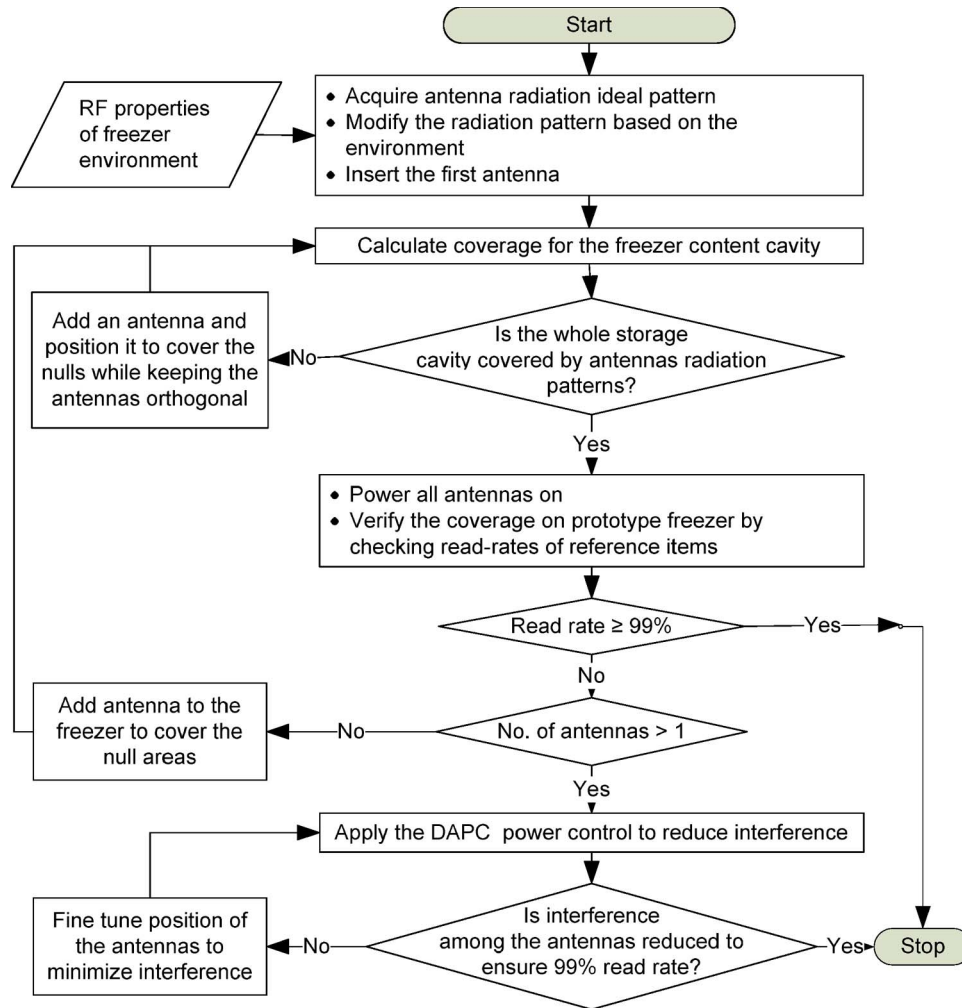$$P_{bs} = K_1 \cdot P_i/r_{i-t}^{4q} = g_{ii} \cdot P_i \quad (20)$$

Fig. 3. Antenna-selection configuration for Missouri S&T smart freezer.

where q is environment-dependent variable considering path loss (depends on stored material properties), r_{i-t} is the distance between reader's antenna and the grid point, and K_1 is the constant that includes reader and tag antenna gains, modulation indexing, and wavelength, as derived in [15]. The gain from the radiation pattern is used to calculate K_1 for each direction. Assuming maximum transmission power $P_{\max}$ and reader's sensitivity level γ, the maximum read range can be calculated from (20) as

$$r_{\max}(\phi) = \sqrt[4q]{G_A(\phi)K_1 P_{\max}/\gamma}$$

where ϕ is the angle around antenna and $G_A(\phi)$ is the reader's antenna gain at an angle ϕ.

Remark 5: In the initial step, a maximum power for each antenna is considered. However, operating the antennas simultaneously at their maximum power will cause collisions among the antennas, thus rendering a significant reduction in coverage and read rates while increasing the read times. As a consequence, DPC is needed to minimize collisions and to ensure the coverage for the given antenna configuration. ∎

The parameter q strongly depends on the environment and has to be determined for a particular type of stored material, operating temperature, etc. For example, when the RF-absorbing

material such as water is used, the attenuation of the RF signal over distance increases, thus reducing coverage and creating nulls. Therefore, more antennas are needed.

2) Selection of Antenna Configuration to Cover the Freezer: The procedure begins with a single antenna. The coverage for the entire freezer is calculated by dividing the freezer volume into a grid of reference points spaced at predefined intervals. For each grid point, the signal strength is calculated from each RFID antenna using the propagation model (20) which includes the absorption properties of the materials.

When the coverage for entire freezer cannot be achieved with maximum antenna power, then additional antennas are added one at a time in orthogonal configuration to cover the nulls. Each antenna is placed to provide best coverage based on their radiation pattern. When a new antenna is added, only the location of this antenna is varied, since the location of the existing antennas had been already established.

Remark 6: The orientation of a tag with reference to antenna alters radar cross section of the tag's antenna. By placing the RFID reader antennas orthogonally, the combined radar cross section will improve, since the maximum value among the considered antennas will apply as

$$C_T(\bullet) = \left\{ \max_i \left(C_i(\phi) \right) \right\}_{\phi=0,\dots,2\pi}$$

where $C_i(\phi)$ is the tag radar cross section for an angle ϕ in reference to ith RFID reader antenna and $C_T(\bullet)$ is combined radar cross section for all RFID reader antennas. ∎

3) Testbed Validation of the Antenna Configuration: The overall performance of the freezer setup is validated on the hardware. The reference tags are placed at worst possible locations (e.g., in the middle of the item stack, at the corner of the designated cavity). The antennas are powered one at a time, and the reference tags are read.

4) Fine Tuning of Antennas' Location to Reduce Interference: Due to limited space inside a freezer, the coverage obtained from steps 1 and 2 will be reduced due to the interference/collisions from other antennas operating simultaneously. Then, the proposed LASDPC scheme or simply DPC is used to minimize the interference while attaining the desired coverage. The DPC selects suitable power while ensuring that there is no overlap in RF coverage among the antennas at all times. This essentially eliminates the collisions among the antennas. The proposed scheme ensures asymptotic stability as presented in Section II-D in contrast with [14], where a bounded stability is shown. This asymptotic stability is needed for attaining 99% read rates and low read times. If the LASDPC alone cannot mitigate the interference, then the antenna position is fine tuned.

Once the consistent 99% read rate is achieved, the current configuration of antennas becomes the solution.

D. Proposed DPC Scheme

In RFID systems, a tag will be detected provided the ratio of the backscatter signal received by the reader is above the target signal-to-noise ratio (SNR) [14]. The SNR is defined as $P_{bs}(k)/I_i(k) > \gamma$, where P_{bs} is the backscatter power from a tag at the time instant k, $I_i(k)$ is the interference at the tag backscatter frequency, and γ is the minimal SNR required to correctly decode the backscatter signal. The SNR state equation for an antenna can now be defined as

$$y_i(k+1) = \theta_i^{\mathrm{T}}(k)\psi_i(k) + P_i(k+1) \cdot \beta_i/I_i(k) \qquad (21)$$

where $y_i(k)$ is the SNR value, $\theta_i^{\mathrm{T}}(l) = [\alpha_i(l) \quad r_i(l)]$ is a vector of unknown parameters, $\psi_i(l) = [y_i(l) \quad \omega_i(l)]^{\mathrm{T}}$ is the regression vector, $P_i(k+1)$ is power at time $k+1$, and β_i is signal loss.

Define the SNR error as $e_i(k) = \gamma - y_i(k)$. By selecting the antenna transmission power as

$$P_i(k+1) = \frac{I_i(k)}{\beta_i^{-1}}\left[- \hat{\theta}_i(k)\psi_i(k) + \gamma_i \right.$$
$$\left. + k_{vi}e_i(k) + \frac{\lambda e_i(k)}{e_i^{\mathrm{T}}(k)e_i(k) + c_i} \right] \qquad (22)$$

where $c_i > 0$ and λ are design constants; one can ensure locally asymptotically stable system. The proposed update law for the channel parameter estimate $\hat{\theta}(k)$ is given by

$$\hat{\theta}(k+1) = \hat{\theta}(k) + \alpha\psi_i e_i^{\mathrm{T}}(k+1). \qquad (23)$$

After combining and defining $\Psi_1(k) = \tilde{\theta}_i^{\mathrm{T}}\psi_i$ and $\varepsilon(k) = \varepsilon_i(k)$, the closed-loop error system in terms of SNR becomes

$$e_i(k+1) = k_{vi}e_i(k) + \Psi_1(k) + \frac{\lambda e_i(k)}{e_i^{\mathrm{T}}(k)e_i(k) + c_i} + \varepsilon(k). \qquad (24)$$

Assume a conic region that satisfies $\varepsilon^{\mathrm{T}}\varepsilon \leq 2\varepsilon_1^{\mathrm{T}}\varepsilon_1 \leq \varepsilon_M = \rho(\|e_i(k)\|)e_i^{\mathrm{T}}(k)e_i(k)$, where $\rho(\|e_i(k)\|) = \lambda^2$, the following theorem guarantees local asymptotic stability of the SNR error dynamics even with channel estimation errors.

Theorem 3 (General Case): Consider the SNR state equation (21) with the parameter update law given by (23) in the presence of bounded channel uncertainties. Let the power update be provided by (22). Then, the SNR error $e_i(k)$ and the channel-parameter estimation errors, $\tilde{\theta}(k)$, respectively, are locally asymptotically stable.

Proof: See the Appendix.

III. SIMULATION AND EXPERIMENTAL RESULTS

A. Simulation Study

In order to verify the effectiveness of the proposed inventory-control scheme, several simulation scenarios were completed in MATLAB. The simulation scenarios depict an industrial shop floor with eight freezers. Actual demand for each freezer was modeled using an assortment of functions, for example, a step function and a sinusoidal function. Demand variation $e_{dij}(k)$ was implemented using a uniform random variable with range $(-10, 10)$. Total error in the inventory level and total delivery request were selected as the performance metrics. The overall goal is to reduce the total error, since high error leads to wastage of materials due to overstocking or disruption of production due to insufficient inventory. Additionally, the total delivery request is observed in order to identify when excess amount of items is ordered.

The proposed scheme is compared with exponential weighted moving-average (EWMA) method [1]. One level of the EWMA smoothing parameter $\alpha = (0.9)$ and two levels of the smoothing parameter $\beta = (0.1, 0.9)$ were tested. Total of three cases were simulated, with and without the DIC scheme and inventory balancing. Each scenario was repeated 500 times, and the results were averaged in order to account for the effects of the stochasticity in the system.

Table I summarizes the results of the simulation study. The proposed scheme performs on par with the best case scenario using EWMA. However, the EWMA parameters need to be manually selected based on experiments [1], since they have a direct effect on the accuracy of the demand prediction. In contrast, the proposed demand-prediction model tunes these parameters online in order to reduce prediction error.

When the DIC backpressure signal is applied, the total error in inventory level is reduced by up to 15% for EWMA and 34% for the proposed scheme over the no-DIC scenario. By employing the backpressure DIC signal, the performance for each demand-prediction scheme is further improved, since the ordering policy for the supply chain compensates for demand

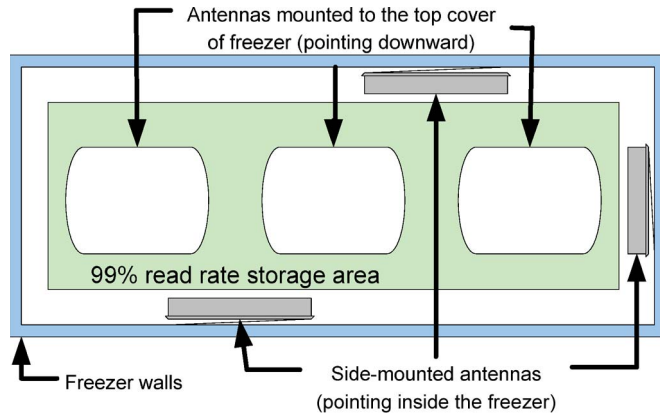|	Proposed Scheme		EWMA $\alpha = 0.9, \beta = 0.1$		EWMA $\alpha = 0.9, \beta = 0.9$	
	Total Error in Inv. Level	Delivery Request	Total Error in Inv. Level	Delivery Request	Total Error in Inv. Level	Delivery Request
No - DIC	15029	25107	11476	24696	12282	24711
DIC w/o Inventory Balancing	9833	24674	9860	24723	10347	24722
DIC w/ Inventory Balancing	2989	24718	2982	24702	3880	25867

Fig. 4. RFID antenna locations for smart-freezer solution.

fluctuations. It is important to note that the main improvement in the performance between EWMA and proposed scheme is the direct result of the online tuning that eliminates the need for offline manual training and can adopt parameters to changing demand patterns without user-intervention. Further performance improvement is observed when all the schemes are implemented with DIC coupled with inventory load balancing. For instance, Table I shows that the DIC with inventory balancing reduces errors in inventory levels by 62%–70% when compared to DIC without inventory load balancing.

B. Hardware Experiments

In the hardware portion of the experimentation, impact of RFID reader and antenna types, number and placement of antennas, reading times, and operational temperature on the read rate were investigated. Each experimental scenario was repeated at least five times to ensure consistency in the results. The containers were kept in the freezer for a prolonged time to study impact of exposure to low temperatures and ice build up.

Placement of antennas inside the freezer that can deliver 99% read rates were identified using the proposed methodology in Section II-C. First, following step 1, the theoretical antenna coverage has been altered to accommodate the presence of ferrous materials inside the freezer. Next, antennas were successively added, and the coverage was tested as per step 2. The intermediate results are shown as follows. The final configuration, as shown in Fig. 4, was achieved by fine tuning the locations of six antennas connected to an Alien ALR9800 reader as per step 4.

The reader was operated with a maximum transmission power of 30 dBm. Tracked items are tagged with Gen-2 tags wrapped around the containers. The proposed LASDPC scheme was implemented at the reader. The antenna-configuration design and confined freezer area resulted in the power-control scheme operating in a simplified on/off mode, where the power control combats the multipath fading alone.

The experimental setup used in this paper is comprised as follows.

1) AR400 Matrics Class 1 Gen 2 RFID reader with dual directional antennas.
2) ALR 9800 Alien Class 1 Gen 2 RFID reader with circularly polarized antennas.
3) The freezer was loaded with 276 containers, including 120 containers with non-RF-friendly (iron oxide) materials. Non-RF-friendly materials absorb the RF signal and negatively affect the overall read rates.
4) AD-220 Gen 2 tags from Avery Dennison were attached to the containers.

Series of experiments have been conducted in order to evaluate the impact of each step of the proposed antenna-configuration design scheme. First, a baseline scenario with simple antenna placement is presented. Next, the steps to determine the desired antenna number and placement are applied, taking into account signal attenuation due to ferrous materials, frost, and tag orientation. Finally, the proposed power control is applied and tested in varying operating conditions. The worst case of -100 °F operating temperature has been thoroughly tested over a period of three months.

1) Results for Antenna Propagation Pattern Calculations: The antenna specification provides basic data about its radiation pattern, including beam width and gains. For example, ALR-9610 circular antenna provides 65° of 3-dB beamwidth. Consequently, the coverage pattern assumes a cone shape that creates nulls for tags located close to antenna but off the beam center. In the proposed design methodology, additional antennas cover the nulls. Second major parameter used in the creation of coverage pattern is the effective read range. The parameters of the model (20) have to be set appropriately for the given environment. Inside a fully loaded freezer, the content can absorb RF signal, thus increasing path loss parameter from $q = 1$ (free space) to $q = 3$ for an iron oxide used in the experiments. Consequently, the read range reduces to 3 ft. Furthermore, the orientation of the tag with respect to the antenna's beam direction can reduce tags gain by up to 3 dB. Based on the read-range model and experimental verification,

TABLE II
PERFORMANCE COMPARISON OF MATRICS AND ALIEN EQUIPMENT

Reader	Antenna	Duration	Read rate		
			1-Antenna	2-Antennas	4-Antennas
Matrics AR-400	AN-100 Dual Directional	180 sec	34-50 %	68-75 %	82-86%
Alien ALR-9800	ALR-9610 Circular	180 sec	59-63%	75-77 %	84-88 %

*Each Matrics antenna include a separate transmitting and receiving element

TABLE III
READ RATES

Reader and Antennas	# of antennas	Duration	Temp. (°F)	No Power Control Random Placement	Power Control Random Placement	Power Control & Antenna Placement
Alien Alr-9800 ALR-9610 Circular	6	40 sec.	20	81%	94%	99%
			-20	80%	93%	99%
			-40	78%	93%	99%
			-60	75%	89%	99%
			-100	73%	88%	99%

the 3-dB loss corresponds to a distance of about 4 in. Hence, the final coverage pattern assumes the shape of a cone with a height of 26 in.

2) Experiments With Various Antenna Configurations: Table II was obtained during the initial testing of RFID-enabled freezer. This paper shows inadequate read rates for simple antenna configuration for both Alien and Matrics antennas. In general, the read rates increase with the number of antennas, since the additional antennas can be positioned to cover the nulls. However, read times appear to be quite high which can be mitigated using DPC, as presented in Table III.

Moreover, the read rates improved for the "multistatic" Alien antennas, since they can switch between transmission and reception, whereas a Matrics antenna includes two static elements. As a result, each Alien antenna acts as two sets of fixed-function antennas, although, physically, there is one. This information should not be confused in the Table II between the manufacturers. Next, the proposed design methodology from Sections II-B–D was applied and experimentally tested.

By using the flowchart shown in Fig. 3, the adequate number of antennas and their location was calculated to be equal to six, and their respective locations are shown in Fig. 4.

Remark 7: The Matrics reader requires that each antenna set contain two elements (transmitter and receiver). Consequently, the complete freezer setup for Matrics reader would require 12 antenna elements, which reduces the storage volume significantly. Hence, Alien readers were only used. ∎

Remark 8: The introduction of antennas into the freezer reduces its volumetric capacity. The actual reduction depends upon the freezer and antenna dimensions. In the proposed freezer (So-Low C85-9 interior: 47 in × 16 in × 20 in), the reduction of the freezer capacity is equal to 28.5% due to 2-in spacing at each freezer wall mounted with antennas. ∎

2) Results for Varying Temperature: The selected antenna configuration was validated at several operating freezer temperatures with proposed antenna placement and power control. The temperature varied from 20 °F to −100 °F, which is a typical range of temperatures used in the composite industry. Table III presents the summary of results. The Missouri S&T scheme renders 99% read rates regardless of freezer temper-

ature, since the methodology ensures coverage in the presence of severe fading and interference while ensuring a low read time of 40 s.

IV. CONCLUSION

This paper has introduced a novel DIC scheme and a methodology to identify the location and number of antennas required for attaining full visibility. The proposed DIC scheme with inventory balancing reduces errors in inventory level when contrasted against a simple demand-prediction scheme. The performance of the DIC scheme was demonstrated through Lyapunov approach. In order to achieve the 99% read rates, the Missouri S&T smart-freezer solution was utilized. The experimental results demonstrate 99% read rates within 40 s at −100 °F temperature with six antennas. Overall, the DIC scheme in concert with the smart-freezer design delivers a reliable and efficient supply-chain solution.

APPENDIX

Proof of Theorem 3: Let the Lyapunov candidate be

$$V = e_i^{\mathrm{T}}(k)e_i(k) + \frac{1}{\alpha}\mathrm{tr}\left[\tilde{\theta}^{\mathrm{T}}k)\tilde{\theta}(k)\right]$$

whose first difference is given by

$$\Delta V = \underbrace{e_i^{\mathrm{T}}(k+1)e_i(k+1) - e_i^{\mathrm{T}}(k)e_i(k)}_{\Delta V_1}$$

$$+ \underbrace{\frac{1}{\alpha}\mathrm{tr}\left[\tilde{\theta}^{\mathrm{T}}(k+1)\tilde{\theta}(k+1) - \tilde{\theta}^{\mathrm{T}}(k)\tilde{\theta}(k)\right]}_{\Delta V_2}$$

$$\Delta V_1 = \left(A_0 e_i(k) + \Psi_1(k) + \frac{\lambda e_i(k)}{e_i^{\mathrm{T}}(k)e_i(k)+c} + \varepsilon(k)\right)^{\mathrm{T}}$$

$$\cdot \left(A_0 e_i(k) + \Psi_1(k) + \frac{\lambda e_i(k)}{e_i^{\mathrm{T}}(k)e_i(k)+c} + \varepsilon(k)\right)$$

$$- e_i^{\mathrm{T}}(k)e_i(k).$$

After mathematical manipulation, ΔV_1 becomes

$$\Delta V_1 = e_i^{\mathrm{T}}(k)A_0^{\mathrm{T}}A_0 e_i(k) + 2e_i^{\mathrm{T}}(k)A_0^{\mathrm{T}}\Psi_1$$

$$+ 2e_i^{\mathrm{T}}(k)A_0^{\mathrm{T}}\frac{\lambda e_i(k)}{e_i^{\mathrm{T}}(k)e_i(k)+c} + 2e_i^{\mathrm{T}}(k)A_0^{\mathrm{T}}\varepsilon + \Psi_1^{\mathrm{T}}\Psi_1$$

$$+ 2\Psi_1^{\mathrm{T}}\frac{\lambda e_i(k)}{e_i^{\mathrm{T}}(k)e_i(k)+c} + 2\Psi_1^{\mathrm{T}}\varepsilon + \frac{\lambda^2 e_i^{\mathrm{T}}(k)e_i(k)}{\left(e_i^{\mathrm{T}}(k)e_i(k)+c\right)^2}$$

$$+ 2\frac{\lambda e_i^{\mathrm{T}}(k)\varepsilon}{e_i^{\mathrm{T}}(k)e_i(k)+c} + \varepsilon^{\mathrm{T}}\varepsilon - e_i^{\mathrm{T}}(k)e_i(k).$$

Next, substituting the parameter update law in ΔV_2 becomes

$$\Delta V_2 = \frac{1}{\alpha}\mathrm{tr}\left[\left(\Delta\tilde{\theta}(k)+\tilde{\theta}(k)\right)^{\mathrm{T}}\cdot\left(\Delta\tilde{\theta}(k)+\tilde{\theta}(k)\right)-\tilde{\theta}^{\mathrm{T}}(k)\tilde{\theta}(k)\right]$$

$$= \frac{1}{\alpha}\mathrm{tr}\left[\alpha^2\varphi\left(e_i^{\mathrm{T}}(k+1)\right)\left(e_i(k+1)\varphi^{\mathrm{T}}\right)\right.$$

$$\left. -2\alpha e_i(k+1)\varphi^{\mathrm{T}}\tilde{\theta}(k)\right]$$

$$= \frac{1}{\alpha}\mathrm{tr}\left[\alpha^2\varphi\left(A_0 e_i(k)+\Psi_1(k)+\frac{\lambda e_i(k)}{e_i^{\mathrm{T}}(k)e_i(k)+c}+\varepsilon(k)\right)^{\mathrm{T}}\right.$$

$$\cdot\left(A_0 e_i(k)+\Psi_1(k)+\frac{\lambda e_i(k)}{e_i^{\mathrm{T}}(k)e_i(k)+c}+\varepsilon(k)\right)\varphi^{\mathrm{T}}$$

$$-2\alpha\left(A_0 e_i(k)+\Psi_1(k)+\frac{\lambda e_i(k)}{e_i^{\mathrm{T}}(k)e_i(k)+c}+\varepsilon(k)\right)$$

$$\left.\times\varphi^{\mathrm{T}}\tilde{\theta}(k)\right].$$

Applying the Cauchy–Schwartz inequality $((a_1 + a_2 + \cdots + a_n)^{\mathrm{T}}\cdot(a_1+a_2+\cdots+a_n) \leq n\cdot(a_1^{\mathrm{T}}a_1+a_2^{\mathrm{T}}a_2+\cdots+a_n^{\mathrm{T}}a_n))$ for the first term in the above equation and applying the trace operator (given a vector $x \in \Re^n$, $\mathrm{tr}(xx^{\mathrm{T}}) = x^{\mathrm{T}}x$)

$$\leq 4\alpha\varphi^{\mathrm{T}}\varphi\left(e_i^{\mathrm{T}}(k)A_0^{\mathrm{T}}A_0 e_i(k) + \Psi_1^{\mathrm{T}}\Psi_1\right.$$

$$+ \frac{\lambda^2 e_i^{\mathrm{T}}(k)e_i(k)}{\left(e_i^{\mathrm{T}}(k)e_i(k)+c\right)^2} + \varepsilon^{\mathrm{T}}\varepsilon\right)$$

$$-2\Psi_1^{\mathrm{T}}\left(A_0 e_i(k)+\Psi_1+\varepsilon+\frac{\lambda e_i(k)}{e_i^{\mathrm{T}}(k)e_i(k)+c}\right).$$

Next, applying $\Delta V = \Delta V_1 + \Delta V_2$ and canceling similar terms, the first difference is given by

$$\Delta V \leq e_i^{\mathrm{T}}(k)A_0^{\mathrm{T}}A_0 e_i(k) + \underbrace{2e_i^{\mathrm{T}}(k)A_0^{\mathrm{T}}\frac{\lambda e_i(k)}{e_i^{\mathrm{T}}(k)e_i(k)+c}}_{1}$$

$$+ \underbrace{2e_i^{\mathrm{T}}(k)A_0^{\mathrm{T}}\varepsilon}_{1} - \Psi_1^{\mathrm{T}}\Psi_1 + \frac{\lambda^2 e_i^{\mathrm{T}}(k)e_i(k)}{\left(e_i^{\mathrm{T}}(k)e_i(k)+c\right)^2}$$

$$+ \underbrace{2\frac{\lambda e_i^{\mathrm{T}}(k)\varepsilon}{e_i^{\mathrm{T}}(k)e_i(k)+c}}_{1} + \varepsilon^{\mathrm{T}}\varepsilon - e_i^{\mathrm{T}}(k)e_i(k)$$

$$+ 4\alpha\varphi^{\mathrm{T}}\varphi e_i^{\mathrm{T}}(k)A_0^{\mathrm{T}}A_0 e_i(k) + 4\alpha\varphi^{\mathrm{T}}\varphi\Psi_1^{\mathrm{T}}\Psi_1$$

$$+ 4\alpha\varphi^{\mathrm{T}}\varphi\frac{\lambda^2 e_i^{\mathrm{T}}(k)e_i(k)}{\left(e_i^{\mathrm{T}}(k)e_i(k)+c\right)^2} + 4\alpha\varphi^{\mathrm{T}}\varphi\varepsilon^{\mathrm{T}}\varepsilon.$$

Now, apply Cauchy–Schwartz inequality $(2ab \leq a^2 + b^2)$ to terms numbered as one in the above equation and using the facts $\varepsilon^{\mathrm{T}}\varepsilon \leq \lambda^2 e_i^{\mathrm{T}}(k)e_i(k)$, $(e_i^{\mathrm{T}}(k)e_i(k)/(e_i^{\mathrm{T}}(k)e_i(k)+c)^2) < e_i^{\mathrm{T}}(k)e_i(k)$, and finally, taking the norm results in

$$\Delta V \leq -\left(1 - 3A_{0\max}^2 - 6\lambda^2 - 4\alpha\varphi_{\max}^2 A_{0\max}^2 - 8\alpha\varphi_{\max}^2\lambda^2\right)$$

$$\times\|e_i\|^2 - \left(1 - 4\alpha\varphi_{\max}^2\right)\|\Psi_1\|^2.$$

Hence, $\Delta V < 0$ if the gains are taken as

$$\alpha \leq 1/4\psi_{i\max}^2 \qquad k_{vi\max} < 1/2$$

$$\lambda = \sqrt{\frac{1 - 3A_{0\max}^2 - 4\alpha\varphi_{\max}^2 A_{0\max}^2}{(6 + 8\alpha\varphi_{\max}^2)}}.$$

This shows that the SNR error $e_i(k)$ and the channel estimation error $\tilde{\theta}(k)$ are locally asymptotically stable.

REFERENCES

[1] M. D. Mills-Harris, A. Soylemezoglu, and C. Saygin, "Adaptive inventory management using RFID data," *Int. J. Adv. Manuf. Technol.*, vol. 32, no. 9, pp. 1045–1051, Apr. 2007.

[2] H. K. H. Chow, K. L. Choy, W. B. Lee, and K. C. Lau, "Design of a RFID case-based resource management system for warehouse operations," *Expert Syst. Appl.*, vol. 30, no. 4, pp. 561–576, May 2006.

[3] X. Lian, X. Zhang, Y. Weng, Z. Duan, and A. Z. Duan, "Warehouse logistics control and management system based on RFID," in *Proc. IEEE Int. Conf. Autom. Logist.*, 2007, pp. 2907–2912.

[4] S. Han, H. Lim, and J. Lee, "An efficient localization scheme for a differential-driving mobile robot based on RFID system," *IEEE Trans. Ind. Electron.*, vol. 54, no. 6, pp. 3362–3369, Dec. 2007.

[5] E. Budak, B. Catay, I. Tekin, H. Yenigun, M. Abbak, S. Drannikov, and O. Simsek, "Design of an RFID-based manufacturing monitoring and analysis system," in *Proc. RFID Eurasia*, 2007, pp. 1–6.

[6] G. Q. Huang, Y. F. Zhang, and P. Y. Jiang, "RFID-based wireless manufacturing for walking-worker assembly islands with fixed-position layouts," *Robot. Comput.-Integr. Manuf.*, vol. 23, no. 4, pp. 469–477, Aug. 2007.

[7] P. Vrba, F. Macurek, and V. Marík, "Using radio frequency identification in agent-based control systems for industrial applications," *Eng. Appl. Artif. Intell.*, vol. 21, no. 3, pp. 331–342, Apr. 2008.

[8] H.-B. Jun, D. Kiritsis, and P. Xirouchakis, "Research issues on closed-loop PLM," *Comput. Ind.*, vol. 58, no. 8/9, pp. 855–868, Dec. 2007.

[9] X. Yang, P. R. Moore, C.-B. Wong, and J.-S. Pu, "A component-based software framework for product lifecycle information management for consumer products," *IEEE Trans. Consum. Electron.*, vol. 53, no. 3, pp. 1195–1203, Aug. 2007.

[10] M. J. Imburgia, "The role of RFID within EDI: Building a competitive advantage in the supply chain," in *Proc. IEEE Int. Conf. Service Oper., Logist. Informatics*, 2006, pp. 1047–1052.

[11] C. Bornhovd, T. Lin, S. Haller, and J. Schaper, "Integrating automatic data acquisition with business processes experiences with SAP's auto-ID infrastructure," in *Proc. Int. Conf. Very Large Data Bases*, 2004, vol. 30, pp. 1182–1188.

[12] R. H. Clarke, D. Twede, J. R. Tazelaar, and K. K. Boyer, "Radio frequency identification (RFID) performance: The effect of tag orientation and package contents," *Packag. Technol. Sci.*, vol. 19, no. 1, pp. 45–54, 2006.

[13] G. G. Yen and L. Ho, "Online multiple-model-based fault diagnosis and accommodation," *IEEE Trans. Ind. Electron.*, vol. 50, no. 2, pp. 296–312, Apr. 2003.

[14] K. Cha, A. Ramachandran, and S. Jagannathan, "Adaptive and probabilistic power control algorithms in dense RFID networks," *Int. J. Distrib. Sensor Netw.*, vol. 4, no. 4, pp. 347–368, Oct. 2008.

[15] M. Fogiel, *The Electronic Communications Problem Solver*. New York: Res. Educ. Assoc., 1988.

Maciej J. Zawodniok (M'03) received the M.S. degree in computer science from Silesian University of Technology, Gliwice, Poland, in 1999, and the Ph.D. degree in computer engineering from Missouri University of Science and Technology, Rolla, in 2006.

Since 2008, he has been with Missouri University of Science and Technology, where he is currently an Assistant Professor of computer engineering in the Department of Electrical Engineering and an Assistant Director of the NSF Industry/University Cooperative Research Center on Intelligent Maintenance Systems. His research focuses on adaptive and energy-efficient protocols for wireless networks, network-centric systems, network security, and cyber-physical and embedded systems with applications to manufacturing and maintenance.

Ahmet Soylemezoglu received the B.S. degree in mechanical engineering from the Eastern Mediterranean University, Famagusta, Cyprus, in 2000, and the M.S. degrees in engineering management and in manufacturing from Missouri University of Science and Technology (formerly the University of Missouri-Rolla), Rolla, in 2001 and 2004, respectively, where he is currently working toward the Ph.D. degree in engineering management with an emphasis on manufacturing engineering in the Department of Engineering Management and Systems Engineering.

His research interests include discrete-event systems, flexible manufacturing systems, shop-floor control, computer integrated manufacturing, preventive maintenance, and shop-floor prognostics.

S. Jagannathan (SM'99) received the B.S degree in electrical engineering from Anna University, Chennai, India, in 1987, the M.S. degree in electrical engineering from the University of Saskatchewan, Saskatoon, SK, Canada, in 1989, and the Ph.D. degree in electrical and computer engineering from the University of Texas at Arlington in 1994.

He is currently the Rutledge–Emerson Distinguished Professor in the Department of Electrical and Computer Engineering and the Site Director for the NSF Industry/University Cooperative Research Center on Intelligent Maintenance Systems, Missouri University of Science and Technology, Rolla. He has coauthored more than 230 archival journal and refereed conference articles, and published several book chapters and three books. He is the holder of 20 patents. His research interests include adaptive and neural-network control, computer/communication/sensor networks, prognostics, and autonomous systems/robotics.